3rd European Supercritical CO2 Conference
September 19-20, 2019, Paris, France

2019-sCO2.eu-149

COOLING SYSTEM COST AND PERFORMANCE MODELS FOR ECONOMIC sCO_2 PLANT OPTIMIZATION WITH RESPECT TO COLD sCO_2 TEMPERATURE

Sandeep R. Pidaparti
KeyLogic
Pittsburgh, PA, U.S.A.

Charles W. White
KeyLogic
Fairfax, VA, U.S.A.

Andrew C. O'Connell
KeyLogic
Pittsburgh, PA, U.S.A.

Nathan T. Weiland*
National Energy Technology Laboratory
Pittsburgh, PA, U.S.A.
nathan.weiland@netl.doe.gov

ABSTRACT

Several studies have shown that the efficiency of sCO_2 power cycles can be significantly improved by reducing the cold sCO_2 temperature, which increases the sCO_2 density at the inlet to the compressor and reduces its specific power requirement. Due to the near-ambient CO_2 critical temperature of 31 °C, the effects of ambient temperature on sCO_2 plant performance are far more significant than for steam Rankine cycles, thus cooling systems tailored to sCO_2 cycle operation are necessary to realize the benefits that are possible through sCO_2 cold temperature management.

To this end, cost and performance models for four different types of sCO_2 cooling systems are presented in this work. These systems cover direct and indirect (via water) cooling of the sCO_2 working fluid, as well as wet and dry cooling techniques to approach ambient wet and dry bulb temperatures, respectively. The heat and mass transfer modeling of these systems are briefly reviewed along with the cost scaling algorithms that have been developed from a combination of literature, cost modeling software, and vendor quotes.

The results of these efforts are a set of sCO_2 cooling system spreadsheet modeling tools that are available for download by the sCO_2 community. The cooling system models can be used by cycle designers to weigh the benefits and drawbacks of various cooling systems in terms of equipment cost, auxiliary power requirements, and water usage. Detailed modeling and capital cost estimation of these cooling systems as a function of ambient conditions and assumed temperature approaches also allows for optimization of the cold sCO_2 temperature to minimize the overall cost of electricity (COE) for a given plant location, accounting for the increased cooling equipment cost required to achieve this temperature. Preliminary economic optimization using these spreadsheet models shows that cooling system optimization improves indirect sCO_2 plant efficiency by 3-4 percentage points, and reduces COE by up to 8%, demonstrating the value and utility of this approach.

INTRODUCTION

A significant feature of the sCO_2-based power cycle is its operation close to the CO_2 critical point (31 °C, 7.37 MPa) towards the cold side of the cycle. For most sCO_2 power cycles, the benefits of reducing the cold sCO_2 heat rejection temperature are particularly advantageous. In this regime, lowering the CO_2 temperature increases its density significantly, reducing the specific power required for compression. Further, lowering the cold sCO_2 temperature allows for an increase in the low temperature recuperator (LTR) effectiveness and also makes the low-grade heat recovery process a more attractive option. Both effects can improve the efficiency of a power plant based on the recompression Brayton cycle (RCBC): the former by directly increasing the power cycle efficiency and the latter by increasing the quantity of heat harvested by the cycle. For similar reasons, the addition of main compressor intercooling typically improves the specific power of a recompression cycle, reducing the sCO_2 mass flow, and thus the required cycle size and cost, for a given power output [1].

To realize the benefits of reduced sCO_2 cycle cold end temperatures, detailed study of the power cycle cooling system is required. Given the close proximity of the CO_2 critical temperature to ambient conditions, sCO_2 cycle cooling system design plays an important role in determining the cold-end cycle performance. However, the capital cost of cooling capacity additions grows exponentially as the sCO_2 cold temperature approaches the design ambient temperature, thus an economic optimum exists that balances the efficiency benefits of cold sCO_2 cycle temperature reductions against the added cooling system expense. Modeling tools for performing such analyses for sCO_2 power cycles are unavailable in the literature, but would allow cycle designers to select the cooling system type, size and operating parameters to economically optimize the plant's interaction with the ambient heat sink.

The objective of this paper is to describe, demonstrate, and make available to the sCO_2 community a set of compact and easy

DOI: 10.17185/duepublico/48915

to use spreadsheet-based models for quantifying the technical (auxiliary power requirement and water usage) and economic (capital and operating costs) performance of four cooling technologies that could be considered for use in sCO_2 power cycle applications. These cooling technologies are:

1. Conventional wet cooling with an evaporative cooling tower.
2. Indirect dry (ID) cooling which uses water-cooled heat exchangers for the sCO_2 power cycle coolers and an air-cooled heat exchanger (ACHE) to reject the cycle waste heat from water to air.
3. Direct dry cooling where each sCO_2 power cycle cooler is an air-cooled heat exchanger directly cooling the CO_2.
4. Adiabatic cooling technology in which the sCO_2 coolers are again air-cooled heat exchangers but the air is cooled below the ambient dry bulb temperature by evaporating water.

These four technologies were selected because they span the gamut of the primary air- and water-cooled technologies that have been considered for the sCO_2 power cycles to date. The models are intended to assist sCO_2 cycle designers in solving three key design questions: at what temperature should the CO_2 coolers be operated for a given ambient temperature, which cooling technology is best for a given application, and what operating conditions are optimal for a given application. To accomplish this, the models give reasonable cooling system designs, complete with techno-economic performance estimates, regardless of the application's geographic location or ambient conditions. This further enables the cycle designer to weigh the capital and operating cost of the selected cooling system against the performance benefits to the sCO_2 cycle.

To provide some context for the discussion below, the modified sCO_2 RCBC shown in Figure 1 is used as a demonstration case for the cooling system economic optimization.

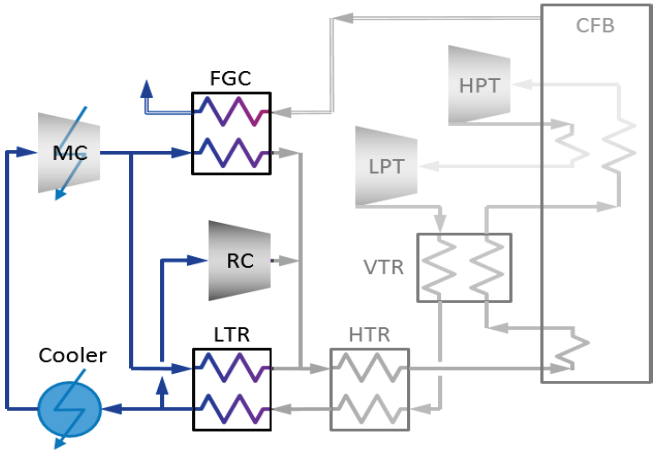

Figure 1: Recompression sCO_2 power cycle

This cycle was modeled using Aspen Plus® (Aspen) in a prior study in which an oxy-coal circulating fluidized bed (CFB) was the primary heat source [1]. From the CFB, the heated CO_2 passes through a turbine (HPT) with one stage of reheat (LPT). The low-pressure CO_2 is then cooled by passing through three stages of recuperators: a very high temperature recuperator (VTR), a high temperature recuperator (HTR), and an LTR. These recuperators in turn heat the high-pressure CO_2 delivered to the CFB. Other cycle types with and without the VTR or reheat have been investigated [1], however, the hot end of the power cycle is shown in gray scale in Figure 1 to focus attention on the subject of this paper - the low temperature portion of the cycle.

After exiting the LTR, the majority of the CO_2 passes through a cooler before being compressed to the peak cycle pressure in the intercooled main compressor (MC) while the rest of the CO_2 enters the recycle compressor (RC). After exiting the MC, the majority of the CO_2 enters the cold side of the LTR where it is partially heated and then mixes with the effluent from the RC. A slipstream of the CO_2 from the MC is heated in a flue gas cooler (FGC) or low temperature economizer before also mixing with the LTR cold side outlet stream.

The original study of the modified RCBC in Figure 1 examined the cost and performance of a baseline coal-fired oxy-CFB power plant with carbon capture [1]. The results showed that the sCO_2 plant offered a significantly higher efficiency and lower cost of electricity (COE) than a plant employing a Rankine cycle at operating conditions similar to the sCO_2 plant. The results also showed that a single stage of intercooling for the main compressor offered both higher overall plant efficiency (0.4 – 0.6 percentage points) and a 1.8 – 2.7% lower COE compared to the baseline configuration. More significant improvements in efficiency (0.6 – 1.6 percentage points) are reported in cases where the pressure ratio between intercooled main compressor stages is optimized [2].

The cold sCO_2 temperature considered in this study was 35 °C, though a preliminary investigation of cold sCO_2 temperatures ranging from 20 – 40 °C for this plant was recently performed [3, 4]. The results show that the plant efficiency increases by about 1 percentage point per 5 °C reduction in cold sCO_2 temperature, accounting for corrections to manage internal pinch points in the FGC, LTR, and cooler for cases with condensing CO_2 and/or main compressor intercooling. A similar efficiency improvement trend with reduction in cold sCO_2 temperature was also encountered in a study of a recompression Brayton cycle plant without CO_2 capture [5, 6].

Several other studies have explored the benefits of reducing the sCO_2 cooler temperature. An early study by Wright *et al.* [7] projected a 4-5 percentage point increase in plant efficiency for a nuclear light water reactor with an sCO_2 power cycle, by moving to condensing cycle operation. An experimental portion of this study proved the feasibility of this concept by demonstrating condensed CO_2 operation of a radial compressor and gas cooler that were designed for gas phase operation near the CO_2 critical point. A later study on sCO_2 power cycles for air-cooled sodium fast reactor nuclear applications showed improvement in cycle performance as the compressor inlet temperature is decreased, as well as variability in performance with compressor inlet pressure [8]. Similar studies in the nuclear application space have shown that an optimal compressor inlet pressure exists for maximizing efficiency as the compressor inlet

DOI: 10.17185/duepublico/48915

temperature is varied. This optimal pressure is typically at [9] or slightly above the pseudo-critical pressure for CO_2 [10].

Pidaparti *et al.* [11] showed the importance of selecting optimum water conditions for the cooling tower to minimize overall plant capital cost for RCBC. Studies comparing the economics of air versus water-cooling have also appeared in the literature. Pidaparti *et al.* performed a detailed study of the economic benefits of air-cooling for the sCO_2 Brayton cycle and found that with a suitable CO_2-to-air cooler design, air-cooling is economically competitive with water-cooling [10]. Held *et al.* performed a comparative analysis of wet cooling versus air cooling for a notional 10 MWe sCO_2 cycle and found that air-cooling will generally be more economically advantageous [12]. Hruska *et al.* performed a life cycle earnings optimization on an air-cooled sCO_2 power cycle compared to a Rankine cycle and found that for the same sized air-cooled heat exchanger, the sCO_2 Brayton cycle can achieve lower heat rejection temperatures than the steam Rankine cycle, which corresponds to higher cycle efficiencies and overall higher life cycle earnings [13].

While some of these studies have presented descriptions of the models and methodologies used to perform their analyses, none have published the actual models. Further, while reliable cost models for dry sCO_2 coolers have recently become available [14], they do not account for variations in cooling system design and operating parameters. The primary contribution of the present study is the development and publication of cost and performance models for four separate cooling system types, which can be used for economic optimization of any sCO_2 plant type with respect to cycle heat rejection to the atmosphere.

COOLING SYSTEM MODELS

This section describes the technical basis of the performance and cost models for all four cooling technologies explored in this study, as well as for water/sCO_2 heat exchangers, where applicable. The cooling technology models, and technical details on their operation and use, can be found in Reference [15]. Wherever possible, the models are compared to data from either commercial software packages or from vendors for validation. All the models operate in design mode only, and do not predict cooling system performance under off-design conditions.

Wet Cooling Tower Performance and Cost Model

The simplest of the cooling technology models in this study uses water/sCO_2 heat exchangers for each of the sCO_2 process coolers and an evaporative wet cooling tower to reject the heat absorbed by the water to the atmosphere. Figure 2 is a schematic diagram for a forced draft wet cooling tower. The warm water exiting the sCO_2 process coolers is collected and fed to the top of the cooling tower where it falls by gravity through a section of packing. Induced draft fans at the top of the tower draw ambient air into the tower through louvers and across the wet packing. As the air passes over the packing, a portion of the water is evaporated, cooling the remaining water. The cooled water is collected at the base of the tower and returned to the CO_2 process coolers via a circulating water pump.

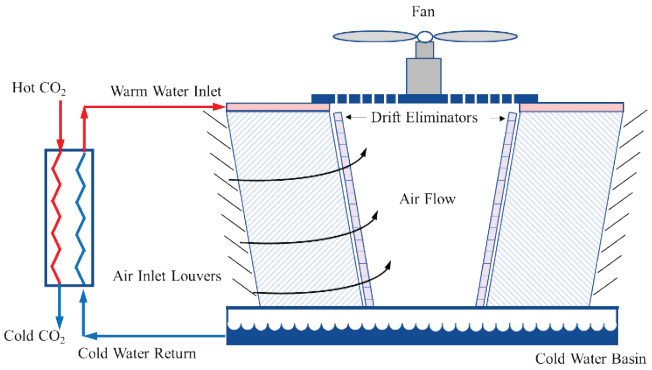

Figure 2: Schematic of the wet cooling tower technology

The central element of the wet cooling tower model is the energy balance that equates the cooling demand of the cooling water with the heat duty of the tower which is the sum of the sensible heat absorbed by the humid air as it passes through the tower plus the latent heat of the evaporated water. The inputs to the model are those typically used to design a wet cooling tower, namely the ambient air conditions (pressure, dry bulb temperature and percent relative humidity or wet bulb temperature), the cold end approach temperature (cold water return temperature minus ambient air wet bulb temperature), the temperature drop (or range) of the water stream, and the inlet water flow rate or total cooling duty. The total water flow rate, m_w, and total cooling duty, Q, are related by:

$$m_w = \frac{Q}{Range * Cp_w}$$

where Cp_w is the average heat capacity of the water. The total amount of water evaporated is obtained from the solution to the overall mass and energy balance and this in turn determines the required air flow rate based on a calculated humidity ratio of the air exiting the tower assuming a hot end approach temperature of 4.7 °C and an assumed relative humidity of 100 percent.

The required fan power is calculated from the required air flow rate, ambient pressure, fan head (default 0.124 kPa) and mechanical efficiency (default 80%). The required power for the circulating water pump is calculated from the total water flow rate, pump head (default 0.254 MPa) and mechanical efficiency (default 80%). The total water loss from the cooling tower is calculated as the sum of the evaporation rate, the blowdown flow rate calculated from the cycles of concentration (default 4) and the entrained water loss or drift loss (default 0.001% of the total water flow rate) [14]. This model has been commonly used in NETL systems studies over the past two decades.

The cooling tower cost algorithm is based on the Zanker correlation, which was presented in a paper by Leeper [15, 16]. This equation estimates the cooling tower construction cost in 1967 dollars with reasonable accuracy based on the total cooling duty, the cooling water range, the cold end approach temperature, and the design ambient wet bulb temperature. Therefore, the Zanker correlation captures the cost impact of various cooling tower design parameters while also accounting for the ambient

DOI: 10.17185/duepublico/48915

conditions available to the tower. Validation of the cost model was performed using the software packages STEAM PRO and PEACE from Thermoflow [17], as shown in Figure 3. In performing the validation, it was determined that the modified Zanker correlation below, incorporating power law scaling for the cooling duty and the cold end approach temperature, results in greater accuracy:

$$\$_{1967} = \frac{Q^o * \left(\frac{Q}{Q^o}\right)^{0.8426}}{C * A^o * \left(\frac{A}{A^o}\right)^{0.4376} + 39.2R - 586}$$

In the modified Zanker correlation, $\$_{1967}$ is the cooling tower construction cost in 1967$, Q is the cooling duty, Q^0 is the reference case cooling duty (3,465 MMBtu/h), A is cold end temperature approach, A^o is the reference case cold end approach temperature (8.52 °F), R is the cooling water range (°F), and C is given by the following equation:

$$C = \frac{279}{[1 + 0.0335 * (85 - Twb)^{1.143}]}$$

where T_{wb} (°F) is the design wet bulb temperature. Cost estimates were converted to 2011$ using the Chemical Engineering Plant Cost Index (CEPCI) [18].

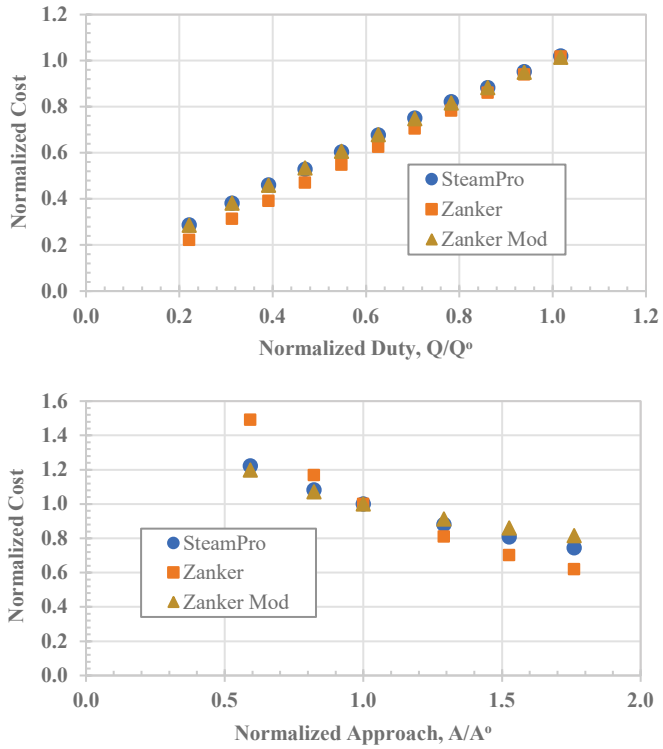

Figure 3: Normalized Cost vs Normalized Duty (top) and Normalized Approach (bottom) for a wet cooling tower

The developed model covers a single cooling tower that is assumed to fulfill the total cooling duty requirements of the plant. The cooling tower approach temperature is assumed to be limited to a minimum of 2.8 °C (5 °F) at the recommendation of cooling tower manufacturers [14].

In the study by Held *et al.* [12], it is noted that the evaporation processes in the wet cooling tower concentrates water impurities, which ultimately may lead to fouling of the water-side of the cycle cooler. If a microchannel heat exchanger is used for the water/sCO$_2$ cooler, then an intermediate high purity water cooling loop is recommended to avoid difficulties with cleaning the intricate flow passages of these heat exchangers. This study assumes a microtube or similar water/sCO$_2$ heat exchanger that is more easily cleaned on the water side, avoiding the need for a secondary heat transfer loop.

Indirect Dry Cooling Performance Model

The schematic of an air-cooled heat exchanger (ACHE) bay and associated water/sCO$_2$ cooler is presented in Figure 4. As depicted in the schematic, a process fluid (water in this case) to be cooled flows through the finned tube heat exchanger bundle (often consisting of multiple rows of tubes and bundles), while fans blow a cold crossflow of air over these bundles. To meet the required cooling duty several such bays can be employed.

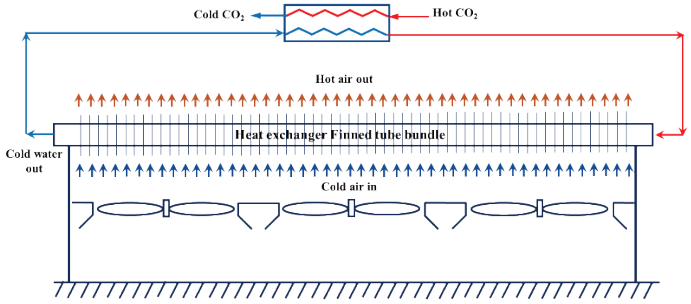

Figure 4: Schematic of the indirect dry cooling technology

The performance model is based on Example 8.1.1 from the textbook by Kröger [19]. The key output variables of the performance model are the number of required bays and the auxiliary fan power consumption to meet the required cooling duty under specified process conditions. The adjustable inputs in the model are cooling duty, CO$_2$ and water fluid parameters (inlet temperature and pressure, outlet temperature), and ambient dry bulb temperature and pressure. The model iteratively calculates the required air flow rate (and fan power), average air outlet temperature, average process fluid flow rate per bay, and the number of required bays.

The implicit energy balance and draft equations are solved iteratively for the main outputs. Closure of the energy balance equations is provided using the ε-NTU relationship. The ε-NTU is feasible and sufficiently accurate for fluids that have only small variation in thermo-physical properties over the temperature range of interest. Effectiveness (ε) of the cross-flow heat exchanger bay is calculated assuming that both the fluids are unmixed. To calculate the NTU, air-side and water-side heat transfer coefficients are needed. The air-side heat transfer coefficient and pressure drop are calculated by assuming that the

DOI: 10.17185/duepublico/48915

tube bundle geometry is the same as the one specified in Example 8.1.1 from the Kröger textbook [19]. The water-side heat transfer coefficient is calculated from the Dittus-Boelter equation, with water properties calculated based on the integrated value between the water inlet and outlet temperatures.

Table 1 shows the design basis and cost estimate for a reference ACHE used as the indirect dry cooler in this application. The cost estimate was prepared by Black & Veatch [20]. This reference indirect dry cooling system cost was converted to 2011$ using the CEPCI [18] and used to determine the bare erected cost (BEC) of a single bay assuming linear scaling. Since the indirect dry model calculates the number of bays required as a primary output, the BEC for any indirect dry cooling configuration is taken as the required number of bays multiplied by the per-bay BEC.

Table 1: Design basis and cost estimate for reference ACHE

Parameter	Value (English Units)	Value (SI Units)
Duty	1820 MMBtu/h	533.4 MW_{th}
Cooling water flow rate	184,000 gpm	41,791 m^3/h
ACHE water inlet temp	89 °F	31.7 °C
ACHE water outlet temp	69 °F	20.6 °C
ACHE outlet temperature approach	10 °F	5.6 °C
Bays required	68	
BEC, $1,000$_{2017}$	80,272	

The approach of using a single per-bay cost value was validated using the results from a series of sensitivity analyses performed in STEAM PRO. Figure 5 shows the cost and number of cells/bays versus the cooling duty, the dry bulb temperature, and the temperature approach. The estimates for the cost and number of cells are from STEAM PRO while the number of bays is scaled from the Black & Veatch reference case. The plots show good agreement between the SteamPro data and the Black & Veatch data. The maximum deviation occurs for an approach below 5.6 °C (10 °F).

In this model, the bay size is governed by the effective frontal area of one tube, which results in modular bay cooling duties between about 15 and 25 MW, depending on approach temperature and range parameters. Approach temperatures below 2.8 °C (5 °F) are not recommended by STEAM PRO, and limits on the range are generally unspecified.

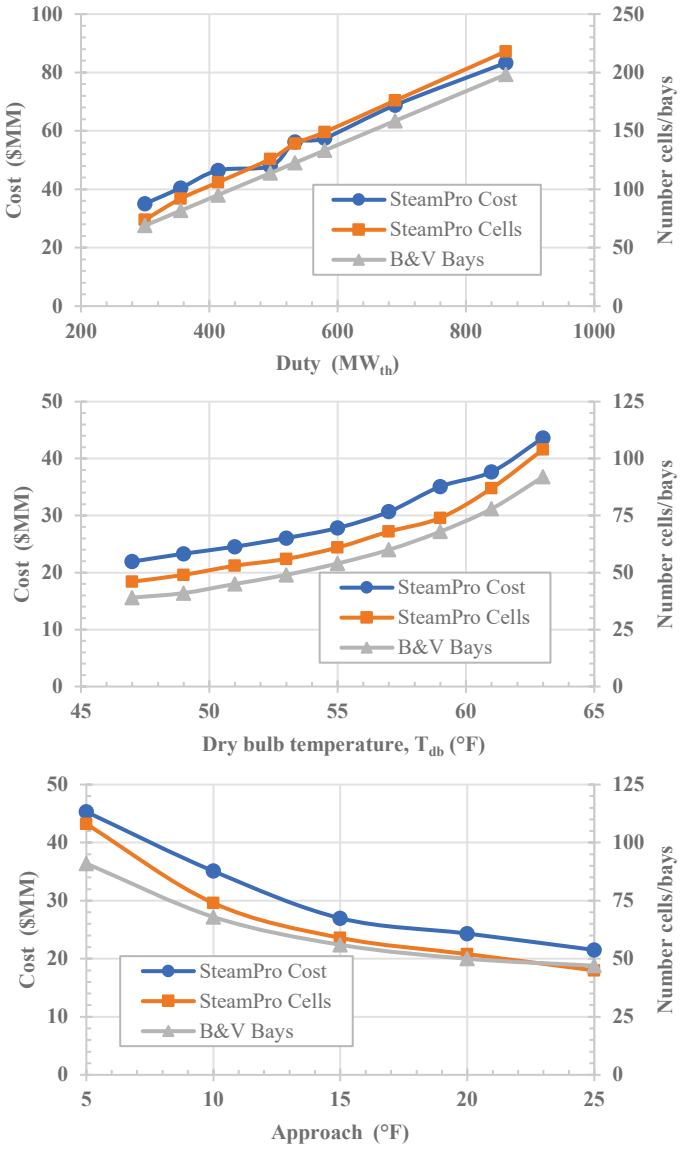

Figure 5: Cost and number of ACHE cells/bays vs. cooling duty, dry bulb temperature and approach temperature

Water-sCO_2 Heat Exchangers

To allow a complete cooling system assessment for the processes using a wet cooling tower or the indirect dry cooling technology, models were developed for the water/sCO_2 coolers required in these systems. For the oxy-CFB indirect sCO_2 cycle system analyzed in this paper, two water/sCO_2 coolers are required, one for the main sCO_2 cooler and the other for the intercooler used in the main CO_2 compressor. Both coolers are modeled as counter-current flow heat exchangers. The thermo-physical properties for both CO_2 and water are calculated using the Span-Wagner equation of state [21] by linking the model to REFPROP [22]. Due to the nonlinear variations in the properties for CO_2, the model discretizes the coolers into 100 segments in the direction of flow. The temperatures and conductance (UA) at each zone are calculated from the energy balance and heat

DOI: 10.17185/duepublico/48915

transfer relations. The minimum temperature approach was determined from an economic optimization to minimize the overall COE. The capital cost model for the water/sCO_2 coolers is identical to that used for the power cycle's low temperature recuperator; \$0.294/(W/K) on a 2011 dollar year basis [15].

Direct Dry Cooling Performance and Cost Models

The schematic of the direct dry CO_2 cooler bay modeled in this study is shown in Figure 6. As depicted in the schematic, CO_2 flows inside finned tube bundles with multiple rows of tubes and passes. The induced draft fans located at the top of the cooler draw cold air over the tube bundles in a crossflow arrangement. Details of the modeled tube bundles are provided in Table 2.

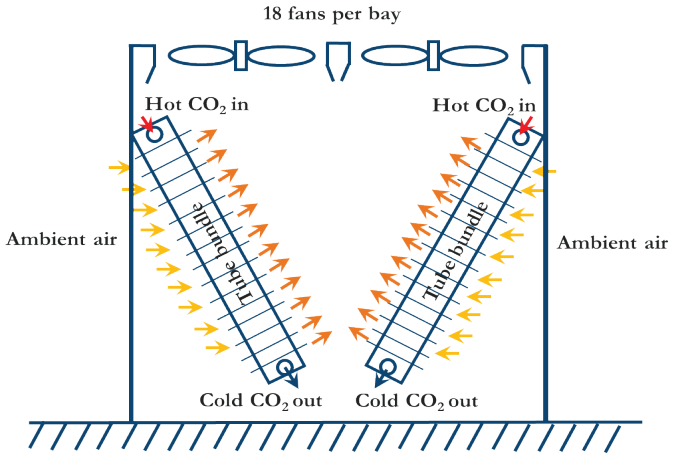

Figure 6: Schematic of the direct dry CO_2 cooler

Table 2: Geometric dimensions of the modeled plate fin-and-tube heat exchanger

Parameter	Value
Tube outer diameter (mm)	12
Tube wall thickness (mm)	0.7
Tube inner diameter (mm)	10.6
Finned tube length (m)	11.385
Tube arrangement pattern	Staggered
Fin thickness (mm)	0.15
Number of tube bundles	2
Number of tubes per row	64
Number of tube passes	3
Number of tubes per pass	2

The performance model is based on Example problems from the Kröger textbook [19]. The adjustable inputs in the spreadsheet are cooling duty, CO_2 operating conditions (inlet temperature and pressure, outlet temperature), air flow rate and ambient dry bulb temperature and pressure. The key output variables of the performance model are the number of required bays and the auxiliary fan power consumption.

The implicit energy balance and draft equations are solved iteratively for the main calculated outputs. Closure to the energy balance equations is provided using the ε-NTU relationship.

The ε-NTU relationship is derived under the assumption of constant properties. This assumption is not valid for CO_2 near the critical point due to the rapidly varying thermo-physical properties in this region. The cooler bay tube bundle is discretized into multiple sub-sections to account for the variation of thermo-physical properties of CO_2. For each sub-section the properties are assumed to be constant and the ε-NTU relationship is applied to each sub-section.

The effectiveness (ε) of each sub-section is calculated using the ε-NTU relationship for cross flow heat exchangers with both fluids unmixed. The air-side heat transfer coefficient and pressure drop across the tube bundle are calculated using the correlations published by Wang *et al.* [23]. For the CO_2-side, a separate set of correlations are used for condensing and non-condensing cases [19]. The CO_2-side heat transfer coefficient and pressure drop for the non-condensing cases are calculated using the Gnielinski correlation [24], while those for the condensing cases are calculated using correlations published by Cavallini *et al.* [25]. According to Cavallini *et al.*, the condensation heat transfer coefficient is either dependent or independent of the difference between the saturation temperature and the wall temperature. Since the wall temperature is unknown *a priori* an iterative algorithm is used to determine the condensation heat transfer coefficient. The frictional pressure drops for the condensing cases are calculated using the correlation of Friedel [26]. The thermo-physical properties for both CO_2 and air are calculated using the Span-Wagner equation of state [21] by linking the Excel spreadsheet to REFPROP [22].

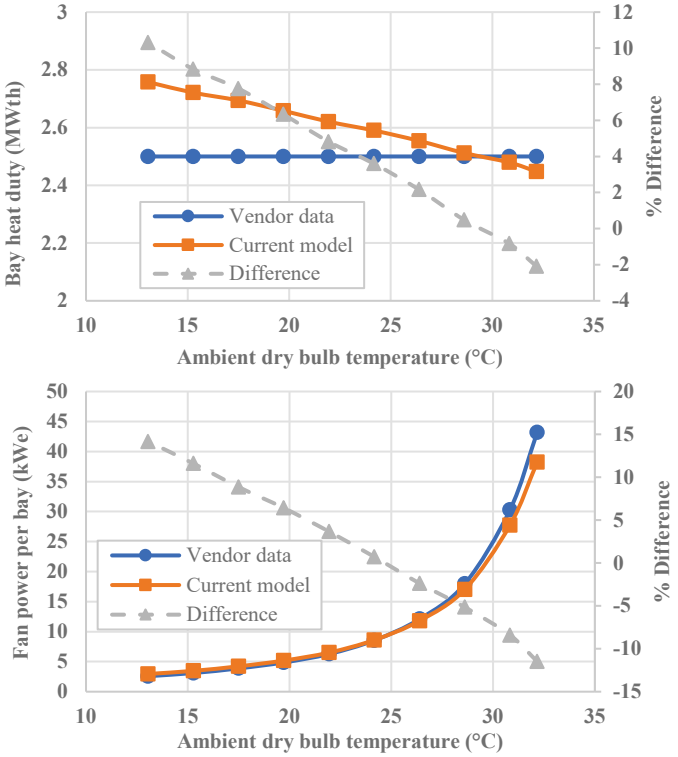

Figure 7: Direct dry cooler bay heat duty (top) and fan power consumption (bottom) as a function of ambient temperature

DOI: 10.17185/duepublico/48915

The performance model was validated against data provided by Guentner, a CO_2 cooler vendor. Figure 7 compares the calculated bay heat duty and fan power consumption from the model and the vendor data. The model was able to predict the vendor data for bay heat duty and fan power consumption within ±10% and ±15% respectively. This accuracy is quite good since the model doesn't fully replicate the vendor tube bundle.

The equipment capital cost of the direct dry cooler is scaled linearly with the number of cooler bays calculated from the performance model. The cost of each cooler bay is determined from the vendor quote. The equipment capital cost is converted to 2011$ using the CEPCI [18]. No further validation of the linear cost model is performed due to lack of reliable data.

Adiabatic Cooling Performance and Cost Model

When the ambient temperatures are high the performance of dry coolers suffer due to approach to the dry bulb temperature. "Adiabatic" cooling systems are used in the CO_2 refrigeration industry to enhance the performance of CO_2 coolers during hot ambient conditions. The schematic of the adiabatic CO_2 cooler bay modeled in this study is shown in Figure 8. The construction of the adiabatic cooler bay is identical to that of direct dry cooler bay from Figure 6, with the addition of pre-cooler pads prior to the tube bundles. These pre-cooler pads are wetted with water when the ambient dry bulb temperature is above a certain set point. As the air is drawn over the wet cooling pads, the air is humidified and cooled to approach the wet bulb temperature. The modeled tube bundles are the same as those of the direct dry cooler from Table 2.

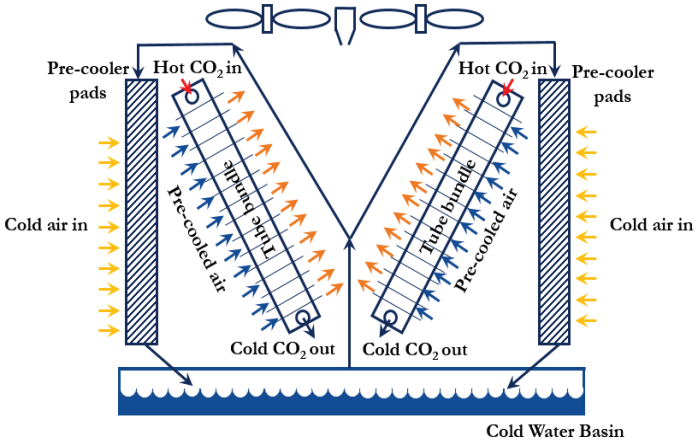

Figure 8: Schematic of the adiabatic cooling technology

The performance model for the adiabatic cooler is broken into two separate models that are executed in series; one for the pre-cooler pad and one for the tube bundle. The pre-cooler pad model solves the simplified mass and energy balance equations between the air and water film in the direction of air flow [27]. The outputs of the pre-cooler pad model are the air outlet temperature, humidity ratio and water consumption rate.

The pre-cooler pad efficiency (approach to wet-bulb temperature), heat transfer coefficient and the pressure drop across the pad depends on the air flow rate and type of the cooling pad. It is assumed that the pad is constructed out of corrugated cellulose paper and the correlations published by S. He *et al.* [27] are used. The outputs from the pre-cooler pad model are provided as inputs to the direct dry cooler bay performance model described in the previous section.

The performance model is validated against data provided by Guentner for their adiabatic CO_2 coolers. Figure 9 compares the calculated bay heat duty, fan power consumption and water consumption between the current model and the vendor data. The model was able to predict the vendor data within ±10%. Again, the accuracy is quite good considering that the pre-cooler pad model and tube bundle model don't fully replicate the vendor design.

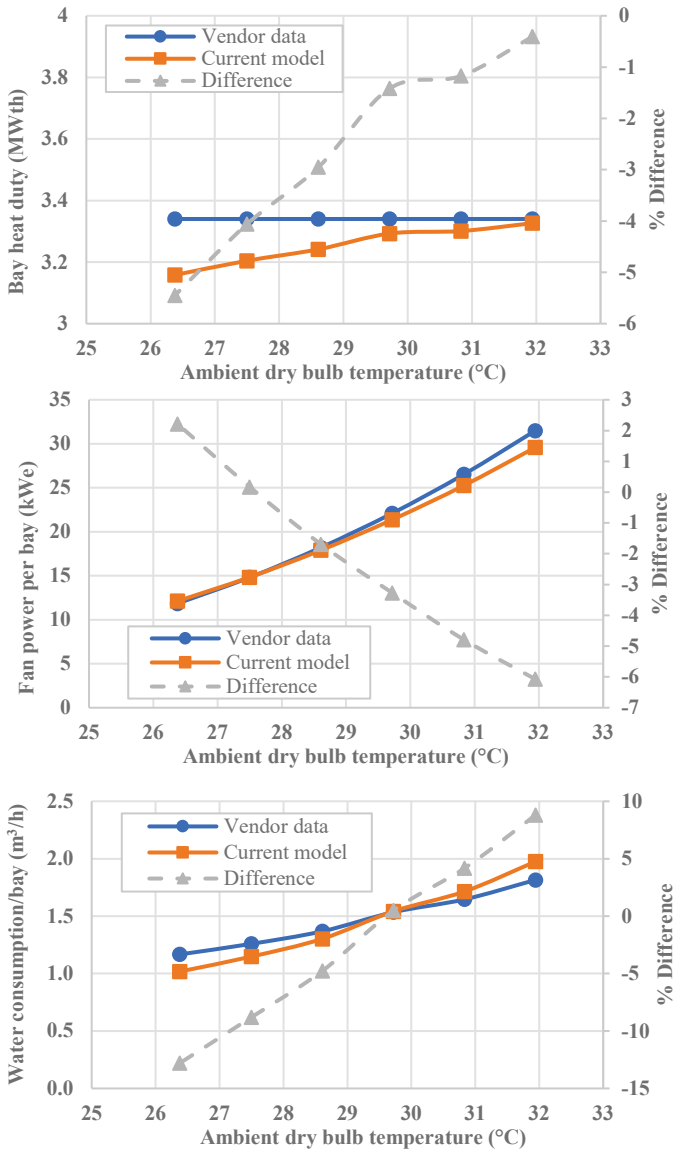

Figure 9: Adiabatic cooler bay heat duty (top), fan power consumption (middle) and water consumption rate (bottom) as a function of ambient dry bulb temperature.

DOI: 10.17185/duepublico/48915

The validated performance model can be used to calculate the number of cooler bays, auxiliary fan power and water consumption as a function of the CO_2 process conditions, cooling duty, ambient air conditions and volumetric flow rate of air.

The equipment capital cost of the adiabatic cooler is scaled linearly with the number of cooler bays calculated from the performance model. The cost of each cooler bay is determined from the vendor quote. The equipment capital cost is converted to 2011$ using the CEPCI [18].

RESULTS AND DISCUSSION

Figure 1 shows a simplified schematic of the RCBC used in this study. A more detailed process flow diagram depicting all of the major plant components as well as a state point table is provided in Reference [1]. As the present work is primarily focused on process sensitivities around the low temperature components of the cycle, the presence or operation of higher temperature cycle components affects the study results only in that they establish a baseline plant efficiency against which these sensitivities are compared.

In modeling the sCO_2 cycle in Aspen, the exit temperatures in the recuperators are determined using design specifications within the model that target a minimum temperature approach at 5.6 °C (10 °F). Similar design specifications are applied to the flue gas and CO_2 coolers.

As a default, the main CO_2 compressor has a single stage of intercooling, although the Aspen model allows a greater number of intercooling stages to be used so that the optimal number of intercooling stages can be determined. In all cases, the intercooler outlet temperature is set equal to the main CO_2 cooler outlet temperature, and the intercooler pressure drop is set to 0.014 MPa (2 psid) for water-cooled cases and 0.14 MPa (20 psid) for air-cooled cases to account for longer sCO_2 pipe runs to the coolers. The isentropic efficiencies and pressure ratios for each compression stage are approximately equal.

The superheat and reheat units, depicted in Figure 1 internal to the CFB, constitute the primary heat exchanger, with each heating the high-pressure sCO_2 stream to the turbine inlet temperature of 760 °C. Two economizers are included in the power cycle to recover additional heat from the flue gas, with the FGC in Figure 1 serving as the flue gas cooler which recovers low quality heat from the flue gas in parallel with the LTR.

Table 3 lists the major assumptions and specifications applied to the RCBC.

Table 3: sCO_2 Brayton cycle model parameters

Parameter	Value
Turbine inlet temperature (°C)	760
Compressor outlet pressure (MPa)	34.6
Intercooler pressure drop (MPa)	0.14 or 0.014
Turbine isentropic efficiency	0.927
Compressor isentropic efficiency	0.85
Cycle pressure drop (MPa)	0.41
Minimum temperature approach (°C)	5.6

Although the focus of this paper is on the cooling system, the following sections show results for the whole plant. The Aspen model yields the performance estimates for the balance of plant components, such as the air separation unit and the CO_2 purification unit. Cost scaling algorithms were used to estimate the capital costs for the non-cooling system components. Details about these performance and cost models along with the methodology used to estimate COE are provided in Reference [1].

The Aspen plant model was run for cooler temperatures of 20, 25, 30, 35, and 40 °C, and the compressor inlet pressure (CIP) that maximizes the cycle and plant efficiency was calculated [4]. It was found that the optimal CIP is slightly higher than the saturation pressure or pseudo-critical pressure, consistent with other studies from literature [10]. The optimal CIP and the maximum cycle efficiency for the five cooler outlet temperatures are summarized in Table 4, where it can be seen that the cooler pressure drop (ΔP_{cooler} of 0.014 MPa vs 0.14 MPa) has no significant effect system performance.

Table 4: Optimal compressor inlet pressure and maximum cycle efficiency as a function of cooler exit temperature

CO_2 cooler temperature (°C)	ΔP_{cooler}=0.014 MPa		ΔP_{cooler}=0.14 MPa	
	Optimal CIP (MPa)	Maximum η_{cycle} (%)	Optimal CIP (MPa)	Maximum η_{cycle} (%)
20	5.86	57.24	5.86	57.24
25	6.55	56.68	6.55	56.67
30	7.45	55.99	7.38	55.92
35	8.34	55.20	8.27	55.20
40	9.31	54.46	9.24	54.39

Although the maximum cycle efficiency increases with decreasing cooler outlet temperature, the capital cost of CO_2 coolers and auxiliary fan power consumption are expected to increase at the same time. Therefore, one would expect a natural trade-off between the efficiency and COE depending on the type of cooling technology and selected parameters for the cooling technology. The four cooling technology performance and cost models described in the previous sections were applied to explore such trade-offs and determine the optimum cold sCO_2 temperature. All presented results assume an ambient pressure of 101.325 kPa, and air dry and wet bulb temperatures of 15 °C and 10.82 °C respectively, corresponding to 60% relative humidity.

Wet cooling tower model results

Figure 10 shows example composite T-Q diagrams for the entire sCO_2 cooling system for the 25 °C (condensing) and 40 °C (noncondensing) cooler temperature cases. In the case of wet cooling technology, cooling tower range ($Range = T_{wi} - T_{wo}$) and approach to the wet bulb temperature ($T_{WCT,app} = T_{wo} - T_{wb}$) are the two independent cooling technology parameters that influence the auxiliary power consumption, capital cost and water consumption rate. The sCO_2 temperatures are fixed by the cycle model, as is the air wet bulb temperature and the hot end air/water approach temperature. For condensing CO_2 cases, 1-D

DOI: 10.17185/duepublico/48915

modeling of the water/CO_2 cooler ensures that a temperature cross does not exist at the point where CO_2 first condenses.

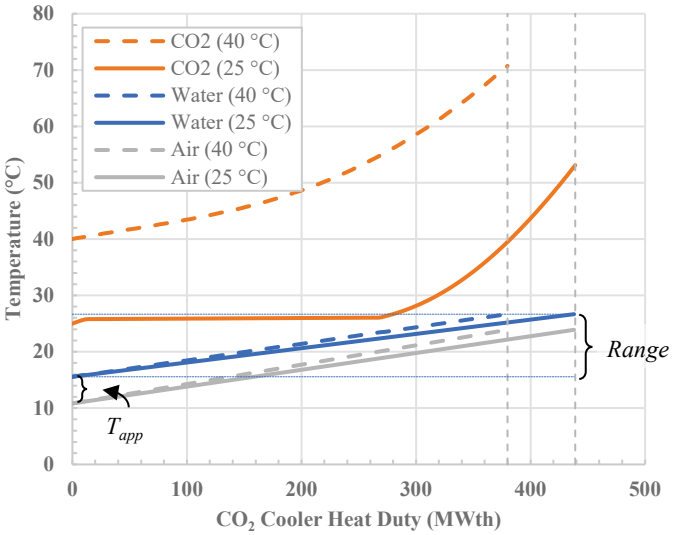

Figure 10: Composite T-Q diagram for the sCO_2 cooling system at 25 °C and 40 °C

Figure 11 shows the COE (without CO_2 transport & storage [T&S] costs) and plant efficiency as a function of cooling tower range and temperature approach for the sCO_2 cooler outlet temperature of 25 °C. For a fixed temperature approach of 2.8 °C (5 °F), the cooling tower range was varied from 5 °C (9 °F) to 20 °C (36 °F). Increasing the cooling tower range impacts the plant efficiency and COE in the following ways: 1) the plant efficiency increases due to a reduction in cooling tower fan and cooling water pump power consumption, 2) the capital cost of water/CO_2 coolers increases due to reduced driving forces and consequently higher heat transfer area requirements, and 3) the capital cost of the cooling tower decreases according to the modified Zanker correlation described earlier. The net impact of these opposing trends on the plant's COE yields a minimum value at a particular value of the cooling tower range (~15.3 °C in this example case).

For the optimum range of ~15.3 °C (27.5 °F), the cooling tower temperature approach was varied from 0 to 11.1 °C (20 °F). Decreasing the cooling tower approach temperature impacts the plant efficiency and COE in the same way as increasing the range as discussed above, except that this leads to a decrease in the water/CO_2 cooler cost due to increased driving forces. The net impact on the plant is that COE attains a minimum value at a low value of cooling tower temperature approach (0.7 °C in this example case). However, as indicated earlier, 2.8 °C was chosen as the minimum cooling tower temperature approach based on recommendation by cooling tower manufacturers. Colder CO_2 cooler temperature cases also optimize to this 2.8 °C temperature approach, though the plant efficiency increases with decreasing temperature approach in these cases. Table 5 shows the optimum values of cooling tower temperature approach and range for each of the cooler exit temperatures. Note that the cooling tower range impacts plant efficiency and COE more than the cooling tower approach temperature, since it affects both water consumption and cooling tower size.

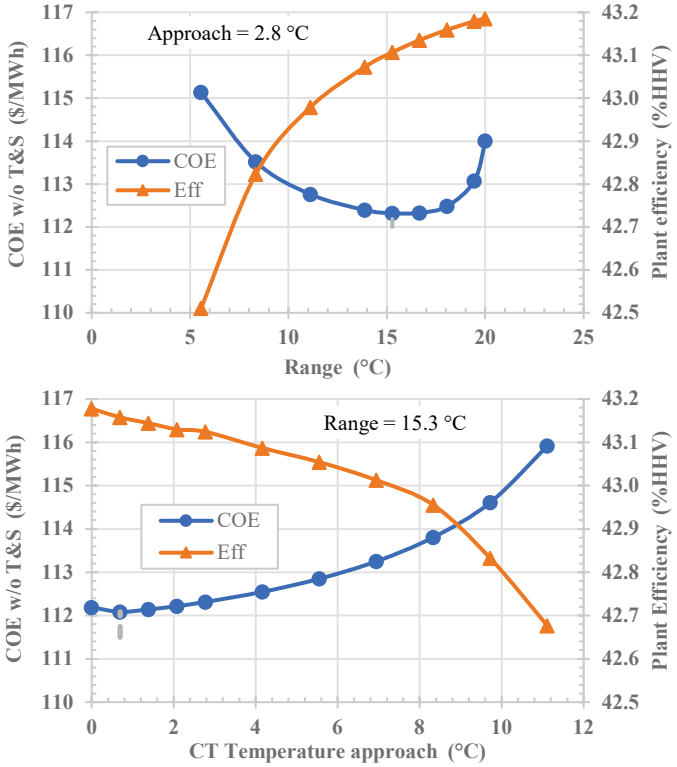

Figure 11: Variation of plant efficiency and COE with respect to cooling tower range and approach temperature.

Table 5: Optimum values of wet cooling tower (WCT) range and temperature approach for each cooler exit temperature

CO_2 cooler temperature (°C)	Optimum WCT approach (°C)	Optimum WCT range (°C)
20	2.8	8.9
25	2.8	15.6
30	2.8	24.4
35	2.8	27.8
40	2.8	27.8

Indirect dry cooling technology model results

In the case of indirect dry cooling technology, the ACHE water range ($Range = T_{wi} - T_{wo}$) and approach to the dry bulb temperature ($T_{app} = T_{wo} - T_{db}$) are the two independent cooling technology parameters that influence the auxiliary power consumption and capital cost. These are analogous to the parameters shown in Figure 10 except T_{app} is the approach to the higher dry bulb temperature. As with the wet cooling tower, the sCO_2 temperatures are fixed by the cycle model, and the inlet air dry bulb temperature is fixed. The hot end air/water approach temperature varies due to the crossflow nature of the ACHE cooler.

Figure 12 shows the COE and plant efficiency as a function of the ACHE range and temperature approach for a cooler outlet temperature of 25 °C. For a fixed ACHE temperature approach

DOI: 10.17185/duepublico/48915

of 2.8 °C (5 °F), the ACHE range was varied from 2.2 °C (4 °F) to 13.3 °C (34 °F). Increasing the ACHE range impacts the plant efficiency and COE as follows: 1) the plant efficiency increases due to reduction in ACHE auxiliary fan power consumption, 2) the capital cost of the water/CO_2 coolers increases due to reduced driving forces and consequently higher heat transfer area requirements, and 3) the capital cost of the ACHE decreases. Due to these opposing trends, the net impact on the plant is that the COE attains a minimum value for a particular value of the ACHE range (approximately 11.1 °C in this example case).

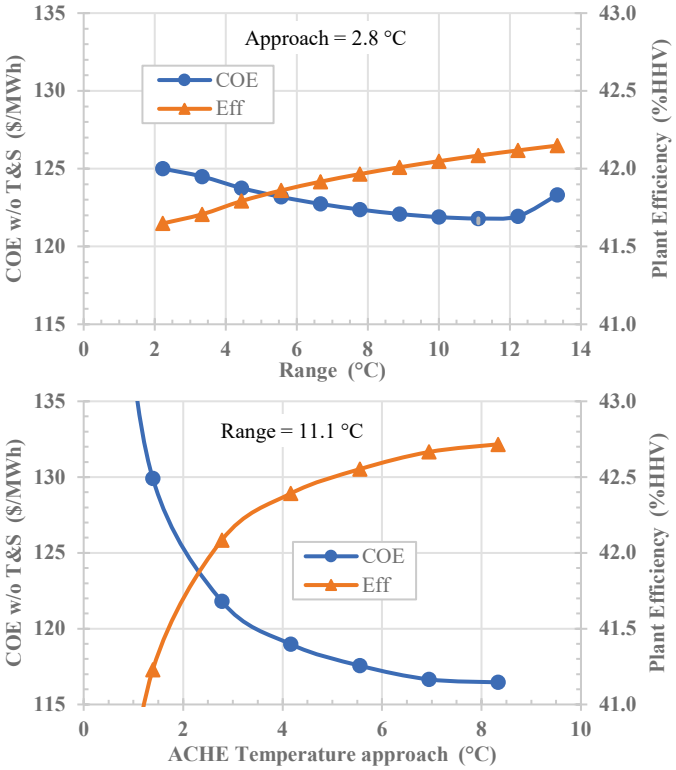

Figure 12: Variation of plant efficiency and COE with respect to indirect dry cooler (ACHE) range and approach temperature

For the optimum range of 11.1 °C (20 °F), the ACHE cooler temperature approach was varied from 0.7 °C (1.3 °F) to 8.3 °C (14.9 °F). Increasing the ACHE temperature approach impacts the plant efficiency and COE in the same manner as increasing the ACHE range, with the minimum COE occurring for larger values of the ACHE temperature approach.

Table 6: Optimum values of Indirect dry (ACHE) temperature approach and range for each the cooler exit temperature

CO_2 cooler temperature (°C)	Optimum ACHE temp. approach (°C)	Optimum ACHE range (°C)
20	4.5	0.37
25	7.9	1.39
30	12.0	3.35
35	16.3	4.75
40	20.1	9.70

Table 6 shows the optimum values of ACHE temperature approach and range for each of the cooler exit temperatures. Note that the optimal cooling system parameters are not general, and only apply to the modeled plant using the economic assumptions applied in its analysis.

Direct dry cooling technology model results

In the case of direct dry cooling technology, the volumetric flow rate of air is the only parameter that influences the cooling duty, auxiliary power consumption, and the capital cost. Figure 13 shows the COE and plant efficiency as a function of the volumetric flow rate of air per bay for a cooler outlet temperature of 25 °C. Increasing the volumetric flow rate of air decreases plant efficiency due to increases in the dry cooler auxiliary fan power consumption, while the number of required cooler bays to meet the design specifications decreases resulting in lower capital cost of the CO_2 coolers. Due to these opposing trends, the COE attains a minimum value for a particular value of air flow rate (approximately 90 m^3/s in this example case).

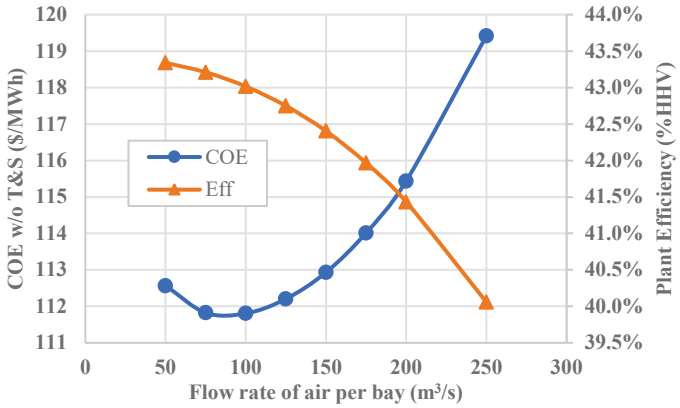

Figure 13: Variation of plant efficiency and COE with respect to flow rate of air per bay for the direct dry cooler

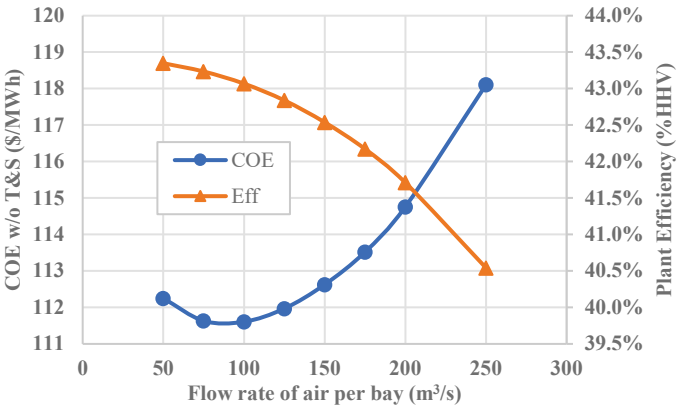

Figure 14: Variation of plant efficiency and COE with respect to flow rate of air per bay for the adiabatic cooler

A similar set of conclusions can be drawn for adiabatic cooling technology as well as depicted in Figure 14. However, in

DOI: 10.17185/duepublico/48915

the case of adiabatic cooling technology the water consumption rate increases with the air flow rate.

Plant COE Optimization Results

Based on the sensitivity analyses presented in the previous sections, the optimum cooling technology parameters are determined for each of the CO_2 cooler temperatures and all four cooling technologies. Figure 15 presents the optimized plant efficiency and COE as a function of CO_2 cooler outlet temperature. Notably, the plant efficiency is shown to improve by 3.0 – 3.5 percentage points, and the plant COE is reduced by as much as 8%, by decreasing the CO_2 cooler temperature from 40 to 20 °C, depending on the cooling technology.

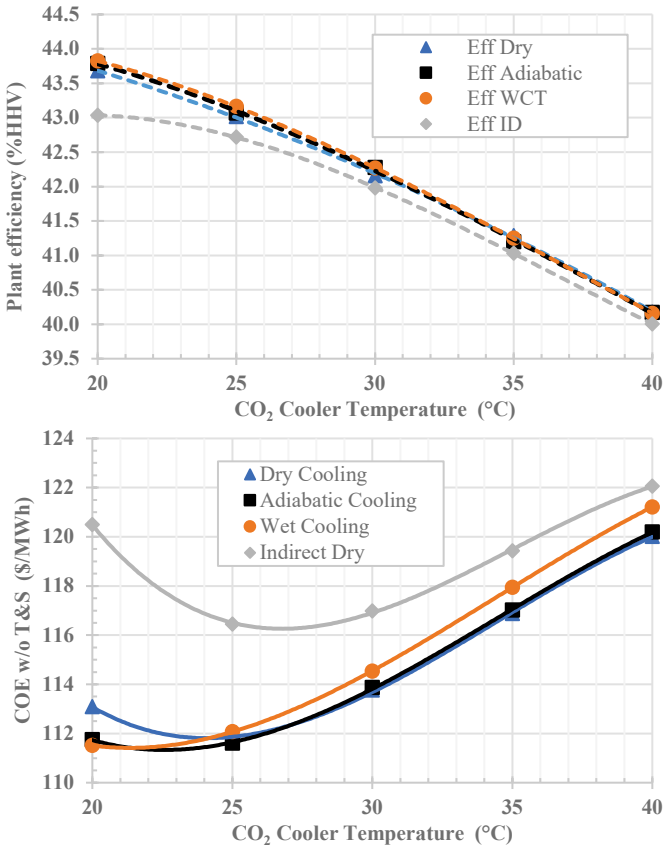

Figure 15: Optimized COE and plant efficiency as a function of cooler outlet temperature for all four cooling technologies

Out of the four cooling technologies, indirect dry cooling technology yields the lowest plant efficiency and highest COE for all the CO_2 cooler temperatures. For CO_2 cooler temperature above 25 °C, both the direct dry cooling and adiabatic cooling technologies offered nearly the same plant efficiency and COE. Moreover, the COE is lowest for the direct dry cooling and adiabatic cooling technologies (relative to other cooling technologies) for CO_2 cooler temperature above 25 °C. The COE of the direct dry cooling technology attains a minimum value for CO_2 cooler temperature of ~25 °C. As the CO_2 cooler temperature decreases below ~25 °C, the COE of the direct dry cooling technology starts to increase due to increases in the capital cost of the CO_2 coolers. It is interesting to note that the COE of the adiabatic cooling technology continues to decrease with CO_2 cooler temperature unlike the direct dry cooling technology.

For the lowest value of the CO_2 cooler temperature investigated (20 °C), the COE of adiabatic cooling and wet cooling tower technologies are similar. However, the water consumption rate in the case of adiabatic cooling technology is significantly lower (689 m^3/h for adiabatic cooling vs 1,146 m^3/h for wet cooling tower). This reduced water consumption makes the adiabatic cooling technology more attractive in hot and dry regions where the water resources are typically scarce. Moreover, unlike the wet cooling tower, adiabatic cooling technology offers the flexibility to operate in dry cooling mode when allowed by low ambient temperatures.

An important point to note is that the optimized results presented here are valid only for the ambient conditions selected. In case of higher/lower ambient temperatures, the optimum cooler temperature will change accordingly for each of the cooling technologies.

CONCLUSIONS & FUTURE WORK

This paper describes the development of performance and cost models for four cooling technologies of interest to indirect sCO_2 power cycle designers, covering both direct sCO_2 cooling and indirect cooling through a water intermediate fluid, as well as wet and dry cooling technologies for approach to ambient wet and dry bulb temperatures, respectively. The models are applicable for any ambient conditions and can thus be used for plant site selection analyses or studies of the expected performance of the system under different climate scenarios. The spreadsheet models are publicly available to the sCO_2 research community to assist in economic optimization of sCO_2 plant designs [15]. While not intended to cover all available cooling technologies, these models do provide a representative cross-section of the various cooling types, all developed with a uniform set of assumptions to allow one to weigh the benefits and drawbacks of each cooling technology type.

Each of the cooling technology models were applied to a pre-existing RCBC model with an oxy-CFB primary heat source to demonstrate their utility in cold-end cycle optimization. Sensitivity analyses show the performance and cost impacts of variations in the design range and approach temperature as well as the air flow rate through the cooling bay for the dry cooling and adiabatic cooling technologies. These sensitivity analyses show the interplay between the overall plant efficiency and COE and generally identify the point of minimum COE.

Finally, a comparative analysis of all four technologies was conducted over a range of CO_2 cooler outlet temperatures between 20 °C and 40 °C. The sCO_2 plant efficiency is shown to improve by 3.0 – 3.5 percentage points, and the plant COE is reduced by as much as 8%, by decreasing the CO_2 cooler temperature from 40 to 20 °C, depending on the cooling technology. This highlights the importance and impact of cooling

DOI: 10.17185/duepublico/48915

system thermal integration for sCO_2 power cycles, and the utility of the spreadsheet models in helping cycle designers develop commercially competitive indirect sCO_2 power systems.

Between the cooling technologies studied, indirect dry cooling has the lowest plant efficiency while wet cooling yields the highest efficiency, with dry cooling and adiabatic cooling only slightly lower. The differences in the impact of CO_2 cooler temperature on efficiency increase as the cooler temperatures approach ambient conditions. The variations in the COE between the four cooling technologies are even more striking. Indirect dry cooling yields the highest COE at all CO_2 cooler temperatures. At the lowest CO_2 cooler temperatures, wet cooling and adiabatic cooling yield the lowest COE while above ~25 °C, direct dry and adiabatic cooling give the lowest COE. Each cooling technology shows a minimum in COE, generally for CO_2 cooler temperatures between 20 °C and ~27 °C.

Work is currently underway to enable use of these spreadsheet cooling models for semi-closed direct sCO_2 power cycles, where the working fluid includes water, oxygen, and other sCO_2 impurities. Future work on the cooling technology models is expected to focus on further improvements in the accuracy of performance and cost estimates through additional vendor data and to increase the number of adjustable design variables for the cooling technologies. These models will be applied to future direct and indirect sCO_2 techno-economic analyses to optimize cooling system designs as a function of plant site ambient conditions, including seasonal temperature variability.

NOMENCLATURE

A	-	WCT cold end temperature approach
ACHE	-	Air-cooled heat exchanger
BEC	-	Bare erected cost
C	-	Zanker correlation coefficient
CEPCI	-	Chemical Engineering Plant Cost Index
CFB	-	Circulating fluidized bed
CIP	-	Compressor inlet pressure
COE	-	Cost of electricity
FGC	-	Flue gas cooler
gpm	-	Gallons per minute
HHV	-	Higher heating value
HTR	-	High temperature recuperator
ID	-	Indirect dry
kWe	-	Kilowatt electric
LTR	-	Low temperature recuperator
m	-	Mass flow rate
MC	-	Main compressor
MWe	-	Megawatt electric
MWth	-	Megawatt thermal
NETL	-	National Energy Technology Laboratory
NTU	-	Number of transfer units
oxy	-	Oxygen
Q	-	Heat duty
R	-	Range
RC	-	Recompression (bypass) compressor
RCBC	-	Recompression Brayton cycle
REFPROP	-	Reference Fluid Thermodynamic and Transport Properties Database
sCO_2	-	Supercritical carbon dioxide
$T_{ACHE,app}$	-	ACHE temperature approach
T_{db}	-	Dry bulb temperature
T-Q	-	Temperature-heat duty
T&S	-	Transportation & storage
T_{wb}	-	Wet bulb temperature
$T_{WCT,app}$	-	Wet cooling tower temperature approach
T_{wi}	-	Inlet water temperature
T_{wo}	-	Outlet water temperature
UA	-	Conductance
VTR	-	Very high temperature recuperator
WCT	-	Wet cooling tower
ε	-	Heat exchanger effectiveness

ACKNOWLEDGEMENTS

The authors wish to thank Richard Dennis (NETL) for his support for this project. The authors also wish to thank Wally Shelton, Travis Shultz (NETL), Mark Woods (KeyLogic) and Eric Lewis, Dale Keairns (Deloitte Consulting, LLP) for their technical assistance and input. Finally, the authors would like to thank Ian Runsey (Guentner), Jamison Ditthardt (Guentner), Tim Leach (Guentner) for providing the vendor data for the dry and the adiabatic cooling technologies. This work was completed under DOE NETL Contract Number DE-FE0004001.

REFERENCES

[1] National Energy Technology Laboratory (NETL), "Techno-economic Evaluation of Utility-Scale Power Plants Based on the Indirect sCO2 Brayton Cycle," DOE/NETL- 2017/1836, Pittsburgh, PA, September 2017.

[2] Y. Ma, M. Liu, J. Yan and J. Liu, "Thermodynamic study of main compression intercooling effects on supercritical CO2 recompression Brayton cycle," *Energy,* vol. 140, pp. 746-756, 2017.

[3] National Energy Technology Laboratory (NETL), "Indirect sCO2 Cycle Cooling Integration for Improved Plant Performance and Cost," DOE/NETL-2018/####, Pittsburgh, PA, January 2018.

[4] N. Weiland, C. White and A. O'Connell, "Effects of Cold Temperature and Main Compressor Intercooling on Recuperator and Recompression Cycle Performance," in *2nd European Supercritical CO2 Conference*, Essen, Germany, August 30-31, 2018.

[5] C. White, W. Shelton, N. Weiland and T. Shultz, "sCO2 Cycle as an Efficiency Improvement Opportunity for Air-fired Coal Combustion," in *The 6th International Supercritical CO2 Power Cycles Symposium*, Pittsburgh, PA, March 27-29, 2018.

DOI: 10.17185/duepublico/48915

[6] National Energy Technology Laboratory (NETL), "Supercritical Carbon Dioxide (sCO2) Cycle as an Efficiency Improvement Opportunity for Air-Fired Coal Combustion," Pittsburgh, PA, February 2019.

[7] S. A. Wright, R. F. Radel, T. M. Conboy and G. E. Rochau, "Modeling and Experimental Results for Condensing Supercritical CO2 Power Cycles," Sandia National Laboratories, Albuquerque, 2011.

[8] T. M. Conboy, M. D. Carlson and G. E. Rochau, "Dry-Cooled Supercritical CO2 Power for Advanced Nuclear Reactors," *Journal of Engineering for Gas Turbines and Power,* vol. 137, pp. 012901-1, 2015.

[9] J. J. Sienicki, A. Moisseytsev and Q. Lv, "Dry Air Cooling and the sCO2 Brayton Cycle," in *Proceedings of the ASME Turbo Expo 2017*, Charlotte, NC, 2017.

[10] S. R. Pidaparti, P. J. Hruska, A. Moisseytsev, J. J. Sienicki and D. Ranjan, "Technical and Economic Feasibility of Dry Air Cooling for the Supercritical CO2 Brayton Cycle Using Existing Technology," in *5th International Symposium - Supercritical CO2 Power Cycles*, San Antonio, Texas, March 28-31, 2016.

[11] S. R. Pidaparti, A. Moisseytsev, J. J. Sienickip and D. Ranjan, "Counter flow induced draft cooling tower option for supercritical carbon dioxide Brayton cycle," *Nuclear Engineering and Design,* vol. 295, pp. 549-558, 2015.

[12] T. J. Held, J. Miller and D. J. Buckmaster, "A Comparative Study of Heat Rejection Systems for sCO2 Power Cycles," in *The 5th International Symposium - Supercritical CO2 Power Cycles*, San Antonio, Texas, March 28-31, 2016.

[13] P. J. Hruska, G. F. Nellis and S. A. Klein, "Methodology of Modeling and Comparing the Use of Direct Air-Cooling for a Supercritical Carbon Dioxide Brayton Cycle and a Steam Rankine Cycle," in *5th International Symposium – Supercritical CO2 Power Cycles*, San Antonio, Texas, March 28-31, 2016.

[14] N. T. Weiland, B. W. Lance and S. R. Pidaparti, "sCO2 Power Cycle Component Cost Correlations from DOE Data Spanning Multiple Scales and Applications," in *ASME Turbo Expo 2019*, Phoenix, Arizona, 2019.

[15] National Energy Technology Laboratory, "Cooling Technology Performance and Cost Models for sCO2 Power Cycles," NETL, Pittsburgh, 2019. https://www.netl.doe.gov/energy-analysis/details?id=3199

[16] SPX Cooling Technologies Inc., Cooling Tower Fundamentals 2nd Edition, Overland Park, Kansas: SPX Cooling Technologies Inc., 2009.

[17] A. Zanker, "Cooling Tower Costs from Operating Data," in *Calculation and Shortcut Handbook*, New York, McGraw-Hill Book Co., 1967, pp. 47-48.

[18] S. A. Leeper, "Wet Cooling Tower: 'Rule-of-thumb' Design and Simulation," Idaho National Engineering Laboratory, EGG-GTH-5775, pp 10-11, 1981.

[19] Thermoflow, *STEAM PRO and PEACE software modules version 27.0,* Southborough, MA: info@thermoflow.com, 2017.

[20] Chemical Engineering, "The Chemical Engineering Plant Cost Index," 2019. [Online]. Available: https://www.chemengonline.com/pci-home.

[21] D. G. Kröger, Air-cooled heat exchangers and cooling towers (Vol. 2), PennWell Books, 2004.

[22] National Energy Technology Laboratory (NETL), "Air Cooled Heat Exchanger (ACHE) Design Final Presentation," Pittsburgh, PA, 2017.

[23] R. Span and W. Wagner, "A New Equation of State for Carbon Dioxide Covering the Fluid Region from the Triple-Point Temperature to 1100 K at Pressures up to 800 MPa," *J. Phys. Chem. Ref. Data,* vol. 25, no. 6, pp. 1509-1596, 1996.

[24] National Institute of Standards and Technology (NIST), *NIST Reference Fluid Thermodynamic and Transport Properties - REFPROP,* U.S. Department of Commerce, 2007.

[25] C.-C. Wang, K.-Y. Chi and C.-J. Chang, "Heat transfer and friction characteristics of plain fin-and-tube heat exchangers, part II: Correlation," *International Journal of Heat and mass transfer,* vol. 43, no. 15, pp. 2693-2700, 2000.

[26] V. Gnielinski, "New equations for heat and mass transfer in turbulent pipe and channel flow," *Int. Chem. Eng.,* vol. 16, no. 2, pp. 359-368, 1976.

[27] A. Cavallini, D. D. Col, L. Doretti, M. Matkovic, L. Rossetto, C. Zilio and G. Censi, "Condensation in horizontal smooth tubes: a new heat transfer model for heat exchanger design," *Heat transfer engineering,* vol. 27, no. 8, pp. 31-38, 2006.

[28] L. Friedel, "Improved friction pressure drop correlation for horizontal and vertical two-phase pipe flow.," *Proc. of European Two-Phase Flow Group Meet., Ispra, Italy,* 1979.

[29] S. He, Z. Guan, H. Gurgenci, K. Hooman, Y. Lu and A. M. Alkhedhair, "Experimental study of film media used for evaporative pre-cooling of air," *Energy conversion and management ,* vol. 87, pp. 874-884, 2014.

DOI: 10.17185/duepublico/48915

DOI: 10.17185/duepublico/48915
URN: urn:nbn:de:hbz:464-20191004-154553-5